Volume 1 | Number 1 | Jan 2013 | Pages 1–100

PCCP

Physical Chemistry Chemical Physics
www.rsc.org/pccp

ROYAL SOCIETY OF CHEMISTRY

ROYAL SOCIETY OF CHEMISTRY

www.rsc.org/pccp

Journal Name

ARTICLE

Ultrafast Spectroscopic and Quantum Mechanical Investigation of Multiple Emissions in Push-Pull Pyridinium Derivatives Bearing Different Electron Donors

B. Carlotti,[a,*] E. Benassi,[b,*] A. Cesaretti,[a] C. G. Fortuna,[c] A. Spalletti,[a] V. Barone[b] and F. Elisei[a]

A joint experimental and theoretical approach, involving state-of-the-art femtosecond fluorescence up-conversion measurements and quantum mechanical computations including vibronic effects, was employed to get a deep insight into the excited state dynamics of two cationic dipolar chromophores (Donor–π–Acceptor$^+$) where the electron deficient portion is a N-methyl pyridinium and the electron donor a trimethoxyphenyl or a pyrene, respectively. The ultrafast spectroscopic investigation, and the Time Resolved Area Normalised Emission Spectra in particular, revealed a peculiar multiple emissive behaviour and allowed distinct emitting states to be remarkably distinguished from solvation dynamics, occurring in water in a similar time scale. The two and three emissions experimentally detected for the trimethoxyphenyl and pyrene derivatives, respectively, were associated to specific local emissive minima in the potential energy surface of S_1 on the ground of quantum–mechanical calculations. A low polar and planar Locally Excited (LE) state together with a highly polar and Twisted Intramolecular Charge Transfer (TICT) state are identified as responsible for the dual emission of the trimethoxyphenyl compound. Interestingly, the more complex photobehaviour of the pyrenyl derivative was explained considering the contribution to the fluorescence coming not only from the LE and TICT states but also from a nearly Planar Intramolecular Charge Transfer (PICT) state, being both the TICT and the PICT generated from LE by progressive torsion around the quasi single bond between the methylpyridinium and the ethene bridge. These findings point to an interconversion between rotamers for the pyrene compound taking place in its excited state against the Non Equilibrated Excited Rotamers (NEER) principle.

Introduction

Non-linear optical (NLO) materials can be very useful for a variety of applications ranging from optical data storage to micro-fabrication, sensing, imaging and cancer therapy facilitated by multiphoton absorption, wherein molecules simultaneously absorb two or more photons.[1,2] Considerable attention has been devoted to organic compounds bearing electron donor (D) and electron acceptor (A) groups linked by π conjugated bridges, as novel, effective and low cost second order NLO and multiphoton absorbing materials.[3-9] It has been observed that the extent of the NLO response and the two photon absorption cross sections are strongly dependent upon the molecular structure of the push-pull molecules and are particularly affected by the strengths of the electron donor/acceptor groups.[10-13] The nature of the electron donor and acceptor portions also significantly alters the spectral

solvatochromism, the photophysical and photochemical behaviour and the efficiency of the photoinduced intramolecular charge transfer of dipolar organic chromophores.[14-18] This effect was observed not only in widely studied neutral donor-acceptor systems but also in cationic chromophores bearing a methyl pyridinium or a methyl quinolinium as electron deficient moiety,[19-24] whose photobehaviour has been less investigated so far and, therefore, not yet deeply understood.

In particular, in a recent paper[19] the effect of solvent polarity on the spectral and photophysical properties of three N-methyl pyridinium dipolar derivatives (where the positively charged pyridinium constitutes the electron deficient and a dimethylamino phenyl, a trimethoxy phenyl and a pyrene the electron rich portion, respectively) was investigated in detail by means of steady-state absorption and fluorescence spectroscopy coupled with nanosecond and femtosecond resolved transient absorption. In principle, these flexible molecules could exist in liquid solution at room temperature as an equilibrium mixture of conformers originating from the rotation around the quasi-single bonds between the aryl groups and the double bond.[25,26] Quantum mechanical (QM) calculations pointed to an equilibrium completely shifted towards the most stable conformer in agreement with the experimental findings.[19] All of the investigated chromophores

a. Department of Chemistry, Biology and Biotechnology and Centro di Eccellenza sui Materiali Innovativi Nanostrutturati (CEMIN), University of Perugia, via Elce di Sotto 8, 06123 Perugia (Italy); email: benedetta.carlotti@gmail.com.
b. Scuola Normale Superiore, Piazza dei Cavalieri 7, 56126 Pisa (Italy); email: enrico.benassi@sns.it.
c. Department of Chemical Sciences, University of Catania, viale Andrea Doria 6, 95125 Catania (Italy).

Please do not adjust margins

show a significant negative solvatochromism of the absorption spectrum, whereas the emission band position is almost unaffected by the solvent polarity. However, an important fluorescence quenching and a shortening of the lifetime of the lowest excited singlet state was observed for the dimethylamino and trimethoxy compounds when passing from low- to high-polarity solvents. A smaller solvent polarity effect was observed in the case of the pyrenyl derivative. Analogously, a change in solvent viscosity under isopolarity conditions caused significant alteration of the fluorescence and excited state properties of the first two push-pull systems, whereas less important modifications of the fluorescence efficiency were retrieved in the case of the third compound even though the excited state dynamics to reach the fully relaxed excited singlet state is significantly slowed down in the more viscous media.

Our latest work,[27] joining state of the art femtosecond fluorescence up conversion spectroscopy and QM computations including vibronic effects, provided a deeper insight into the excited state dynamics of the dimethylamino methylpyridinium derivative, the widely used dye o-DASPMI (compound **1** in Chart 1), unravelling a dual emission behaviour, not yet unanimously accepted in the literature for negatively solvatochromic systems. The ultrafast fluorescence measurements (and the Time Resolved Area Normalised Emission Spectra analysis in particular) indeed allowed to identify the presence of two distinct emitting species, characterised by similar emission energies, and to distinguish their population dynamics from simple relaxation processes, such as solvation. The QM calculations provided a detailed description of the two emitting minima in the potential energy surface (PES) of the first excited singlet state (S_1): the locally excited (LE) minimum, characterised by a planar geometry and a low dipole moment and the twisted intra-molecular charge transfer (TICT) minimum, highly polar and formed from LE by torsion around the quasi-single bond adjacent to the pyridinium ring. Such interesting results prompted us to extend, through the present work, the promising approach of combined experimental and theoretical investigations to the study of the excited state dynamics of the two other push-pull cationic chromophores differing in the electron donor portions (compounds **2** and **3** in Chart 1), with the existence of a multiple emission behaviour for these charged dyes being rarely and controversially discussed in the literature.[28-32]
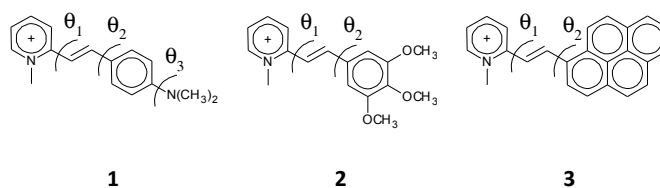
Chart 1. Chemical sketch of the most stable conformer[19] of compounds **1**, **2**, and **3**, with definition of the dihedral angles of interest.

Results and discussion

Fluorescence up-conversion experiments proved revealing, allowing a deep comprehension of the excited state dynamics of compounds **2** and **3** in water. The time resolved emission spectra of **2** (Figure 1, left graph panel B) right after laser excitation are centred around 500 nm and undergo a significant bathochromic shift over time up to about 550 nm, eventually matching the position of the stationary fluorescence spectrum (see Table 1). The kinetics recorded in the blue portion of the investigated spectral range are dominated by a fast decay whereas those acquired in the long wavelength region exhibit a fast rise followed by a slower decay. The Target Analysis of these data revealed the presence of three exponential components characterised by lifetimes of 0.20, 1.1 and 28 ps and Species Associated Spectra (shown in panel C of Figure 1, left graph) centred at 500, 525 and 550 nm, respectively. The obtained lifetimes are in good agreement (within the experimental error) with those previously retrieved by means of femtosecond transient absorption measurements for the same compound in water (0.24, 0.91 and 25 ps, respectively).[19] The first two components were previously ascribed to the possibility of distinguishing the ultrafast inertial solvation component ($\tau_1 \approx$ 0.2 ps) from the slower diffusional solvation component ($\tau_2 \approx 1$ ps)[33,34] whereas the longest transient ($\tau_3 \approx 25$ ps) was assigned to the fully relaxed excited singlet state. This behaviour is slightly different from that of the single subpicosecond exponential component of 0.5 ps and the shorter living S_1 observed for compound **1** in the same solvent (see Table 1).[19] The application of the *TRANES* analysis in the present work played a crucial role in getting a more profound insight into the nature of the three transients observed for **2** (Figure 1, right graph).

Table 1. Experimental results obtained by steady state absorption (Abs), emission (Em) and Fluorescence Up-Conversion (FUC) measurements of compounds **1**, **2** and **3** in water.

	Abs	Em	FUC					
	λ_{max}/ nm	λ_{max}/ nm	$\lambda_{max,1}$/ nm	τ_1 /ps	$\lambda_{max,2}$/ nm	τ_2 /ps	$\lambda_{max,3}$/ nm	τ_3 /ps
1[a]	438	589	565	0.51	595	4.8		
2	353	546	480	0.20	525	1.1	550	28
3	390[sh],420	586	550	1.0	585	40	585	270

[a] from ref. 27
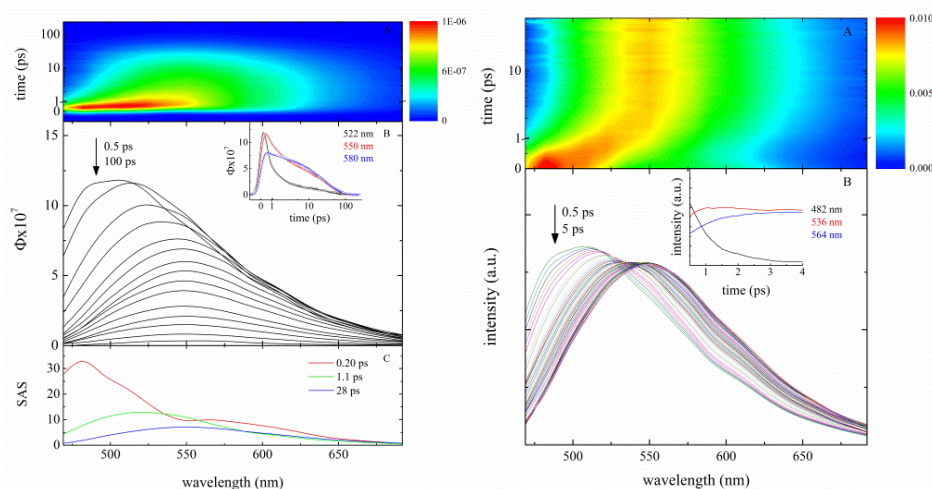
Figure 1. Fluorescence up–conversion (λ_{exc}=400 nm) of **2** in water. Left graph: A) contour plot of the experimental data, B) time resolved emission spectra recorded between 0.5 and 100 ps after the laser pulse. Inset: decay kinetics recorded at meaningful wavelengths together with the corresponding fitting traces and C) SAS of the decay components obtained by Target Analysis. Right graph: A) contour plot of the *TRANES* and B) their spectral evolution recorded between 0.5 and 5 ps after the laser pulse. Inset: time–profile of the *TRANES*.
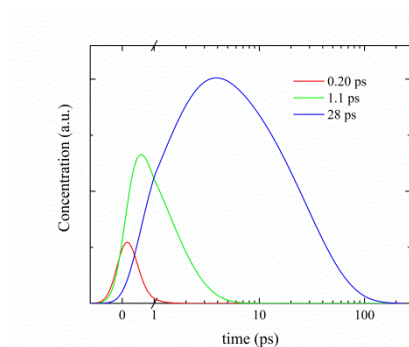
Figure 2. Concentration profiles of the various transients obtained from the Target Analysis of the fluorescence up-conversion data of **2** in water.

During the first hundreds of femtoseconds after the excitation, the continuous *TRANES* shift accounts for the solvent equilibration around the excited state in the Franck-Condon region.[35] However, after the first picoseconds, an isosbestic point appears around 550 nm, *videlicet* when the shortest transient has fully decayed and only two emitting species are present in solution (cf. concentration profiles, Figure 2): the 1 ps state, emitting at 525 nm, and the 28 ps state, emitting at 550 nm and mainly responsible for the steady-state fluorescence (see Table 1). As is the case with **1**,[27] the spectral separation of these two states is not large enough to provide evidence of their interplay in the steady-state spectra: no solvatochromic effect was indeed revealed in the stationary emission spectra of **2** recorded in solvents of different polarity.[19] It is noteworthy to point out that the excited state dynamics is slower for **2** than for **1** and, since the latter compound bears a stronger electron donor group and the same electron deficient N-methyl pyridinium portion, the

transient behaviour might be dominated by the occurrence of ICT processes. Compound **2** gets stabilised by inertial solvation into the first emissive state, which later evolves into the second state according to the time constant of diffusional solvation (about 1 ps) and thus together with it, while the photoinduced evolution takes place in the excited state of **1** within the faster component of solvation, being mixed with it and hence occurring in the sub-picosecond time scale.

The excited state dynamics of the pyrenyl derivative **3** in water shows peculiar features with respect to the other N-methylpyridinium salts. Even though slightly red-shifted, its time resolved emission spectra look similar to those of the other two compounds (Figure 3, left graph panel B). The fluorescence up-conversion data of **3** were properly fitted with three components (τ = 1.0, 40, 270 ps), in conformity with the three longest transients previously revealed by ultrafast Excited State Absorption (ESA) measurements (τ = 0.1, 1.1, 20 and 275 ps).[19] The non-detectability of the ultrafast component associated with inertial solvation might be owed to the reduced resolution of the up-conversion equipment with respect to that of the ESA apparatus. Surprisingly, the *TRANES* evolution reveals the presence of a net isoemissive point around 580 nm (Figure 3, right graph panel B), already formed at early delays, that is to say during the solvation stage. The isosbestic point is kept within the first ten picoseconds, until the concentration of the longest component grows large enough to contribute to the emission spectra (Figure 4). At longer delays, the *TRANES* (Figure 5) undergo a slight enhancement in intensity and an apparent decrease in width on the red side of the spectrum and a second quasi-isosbestic point is observed around 625 nm. These findings pushed us to consider the involvement of a third state in the deactivation of **3**, since the number of isosbestic points (*n*) in the *TRANES* evolution is related to the number of emitting species by the relation *n+1*.[35]

It would thus seem entirely reasonable to speculate upon a three-state decay pattern for **3** defined as follows: the 400 nm laser radiation excites the molecule to a first state which emits around 550 nm and decays to a second state emitting at 585 nm within the diffusive solvent equilibration ($\tau_1 \approx 1$ ps).[33,34] From this stage the deactivation ($\tau_2 \approx 20\text{-}40$ ps for **3**) implies the formation of a third state ($\tau_3 \approx 270$ ps), whose fluorescence is still centred at about 585 nm and perfectly matches the steady-state emission spectrum (see Table 1). By employing

the Target Analysis, attempts were made to globally fit the experimental data using a parallel branched kinetic model rather than a consecutive one, but worse results were achieved in terms of goodness of the obtained fit in reproducing the experimental behaviour. We therefore believe that the three emissive states revealed during the deactivation of the pyrenyl derivative are effectively reached in succession after light absorption.
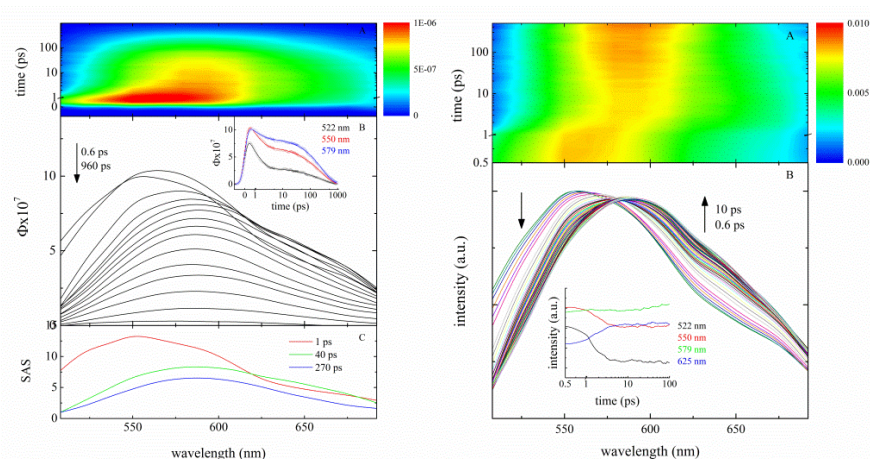
Figure 3. Fluorescence up–conversion (λ_{exc}=400 nm) of **3** in a water/ethanol mixture 90/10 v/v. Left graph: A) contour plot of the experimental data, B) time resolved emission spectra recorded between 0.6 and 960 ps after the laser pulse. Inset: decay kinetics recorded at meaningful wavelengths together with the corresponding fitting traces and C) SAS of the decay components obtained by Target Analysis. Right graph: A) contour plot of the *TRANES* and B) their spectral evolution recorded between 0.6 and 10 ps after the laser pulse. Inset: time–profile of the *TRANES*.
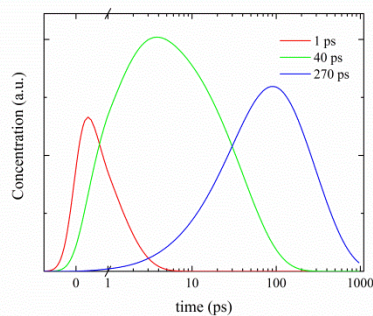
Figure 4. Concentration profiles of the various transients obtained from the Target Analysis of the fluorescence up-conversion data of **3** in a water/ethanol mixture 90/10 v/v.

A mechanistic interpretation of the experimental observations was found by vibronic computations based on DFT and TD-DFT potential energy surfaces of the key electronic states including bulk solvent effects by means of the PCM. The optimised geometries retrieved for the ground state single minimum and the different S_1 local minima of compounds **2** and **3** in aqueous solution are shown in Figure 6, together with those previously obtained for compound **1**.[27] The ground state geometries for both compounds are slightly distorted from planarity, exhibiting dihedral angles (θ_1 for **2**; both θ_1 and θ_2 for **3**, see

Chart 1) of about 30°, because of small rotations around the quasi-single bonds between the aromatic rings and the ethene bridge (see Table 2). Conversely, the LE (locally excited) local minimum is characterised by a strictly planar structure and a dipole moment (μ_{LE} = 6.22 D for **2** and 3.46 D for **3**) similar to that of the Franck-Condon state and significantly weaker than that of the corresponding ground state (μ_G = 19.79 D for **2** and 15.12 D for **3**, see Figure 7). The LE states of both **2** and **3** are highly emissive, with their fluorescence being characterised by oscillator strengths around 1.5.
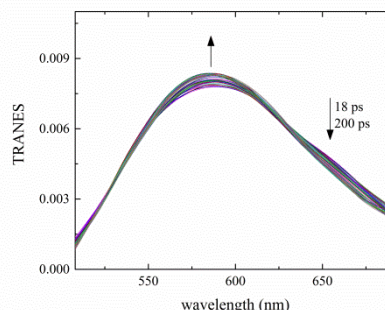
Figure 5. Spectral evolution of the *TRANES* recorded between 18 and 200 ps after the laser pulse for **3** in a water/ethanol mixture 90/10 v/v.

Other twisted and planar local minima (TICT and PICT) of the lowest excited singlet state, all characterised by high dipole moments (see Figure 7) and therefore obtained by intra-molecular charge transfer processes, were found by considering the possible torsions around the dihedral angles θ_1 and θ_2 (in the case of compound **1**, an additional possible torsion around θ_3 can also be considered[27] as depicted in Chart 1). The structural and electronic properties of these local minima are displayed in Figure 6 and 7, respectively. Unlike what found for **1**,[27] in the case of **2** and **3** the torsion around the dihedral angle θ_1 (the one adjacent to the N-methyl pyridinium moiety) originates two stable minima in the excited state PES, namely TICT1 and PICT1, the former showing a twisted and the latter an almost planar geometry (see Table 2). As is the case with **2** and just like what was previously retrieved for **1**, only TICT1 has a significant oscillator strength[27] whilst for **3** both TICT1 and PICT1 show non-negligible emission probability. PICT1 is at the same time less stable and less polar than TICT1. The emission energies of these two minima are close to each other and lower that the LE emission energy. As already observed for **1**,[27] also in the case of **2** and **3** TICT2, generated by rotation around θ_2, represents a non-emissive minimum.

In the case of compound **2**, the two emissive species revealed by means of the fluorescence up-conversion measurements, characterised by lifetimes of 1.1 and 28 ps, correspond to the two local minima in the S_1 state: the LE and TICT1 minima found at the TD-DFT level. A very good agreement was also found between the experimentally observed and theoretically predicted emission energies (see Table 1 and Figure 7; the computed energies are those corresponding to the maximum of the spectral band obtained after the convolution of the stick vibronic spectrum). In the case of compound **3**, the three consecutive fluorescent transients resulting from the ultrafast measurements are related to the three calculated emissive minima LE, TICT1 and PICT1. The last two minima (TICT1 and PICT1) are reached from the planar LE structure by progressive

θ_1 torsions of about 90° and 150°, respectively. PICT1 therefore involves a low-stability conformer, practically absent in the ground state,[19] which becomes indeed nearly iso-energetic with LE in the lowest excited singlet state. It is remarkable that this different conformational equilibrium in S_1 contradicts the NEER (Non Equilibrated Excited Rotamers) principle, as already observed for some other flexible molecules.[26,36] Both experiments and theory indicate that the emission energy of the low polar LE minimum is higher than that of the two ICT minima, which show similar emission energies, being both characterised by significant dipole moments.

The findings of the present work allowed us to gain a deeper understanding of the behaviour of **2** and **3**, that is their solvent-dependent photophysics and excited state dynamics reported in ref. 19. The fluorescence quantum yields of compound **2** result significantly influenced by changes in both solvent polarity and viscosity, whereas a much smaller effect was observed in the case of compound **3**. This different behaviour is in full agreement with the fact that the longest living species in S_1, the one probably giving the most important contribution to the stationary emission, shows a twisted conformation in the case of compound **2** and a planar geometry in the case of **3**. Interestingly, the up-conversion measurements combined with DFT/TD-DFT calculations including vibronic effects allowed the presence of an additional emissive component to be evidenced in the case of the pyrenyl derivative with respect to those previously inferred from ESA measurements.[19] Furthermore, some dependence on the solvent viscosity for the lifetimes of the species revealed during previous femtosecond transient absorption measurements for both **2** and **3**[19] is comprehensible considering the progressive torsions taking place in the excited states of both compounds. Interestingly, the transient which is less affected by increasing solvent viscosity is the longer living PICT1 state of **3**[19] supposedly owing to its nearly planar geometry.

Table 2. Dihedral angles (in degrees) of the optimised geometries of G and ES (LE, TICT1, PICT1, TICT2 and TICT3) minima of compounds **1**, **2** and **3** in water. Level of theory: (TD-)DFT CAM-B3LYP/SNSD/IEF-PCM(UFF).

	1[a]			**2**		**3**	
	θ_1 / degs	θ_2 / degs	θ_3 / degs	θ_1 / degs	θ_2 / degs	θ_1 / degs	θ_2 / degs
G	179.6	179.9	180.0	151.2	170.6	152.3	154.4
LE	180.0	179.9	180.0	179.9	179.7	180.0	180.0
TICT1	103.8	177.3	179.2	84.9	175.2	89.2	172.5
PICT1	-	-	-	24.8	174.6	29.5	171.1
TICT2	179.9	90.7	179.9	178.6	90.3	174.4	89.1
TICT3	179.8	180.0	90.5	-	-	-	-

[a] from ref. 27
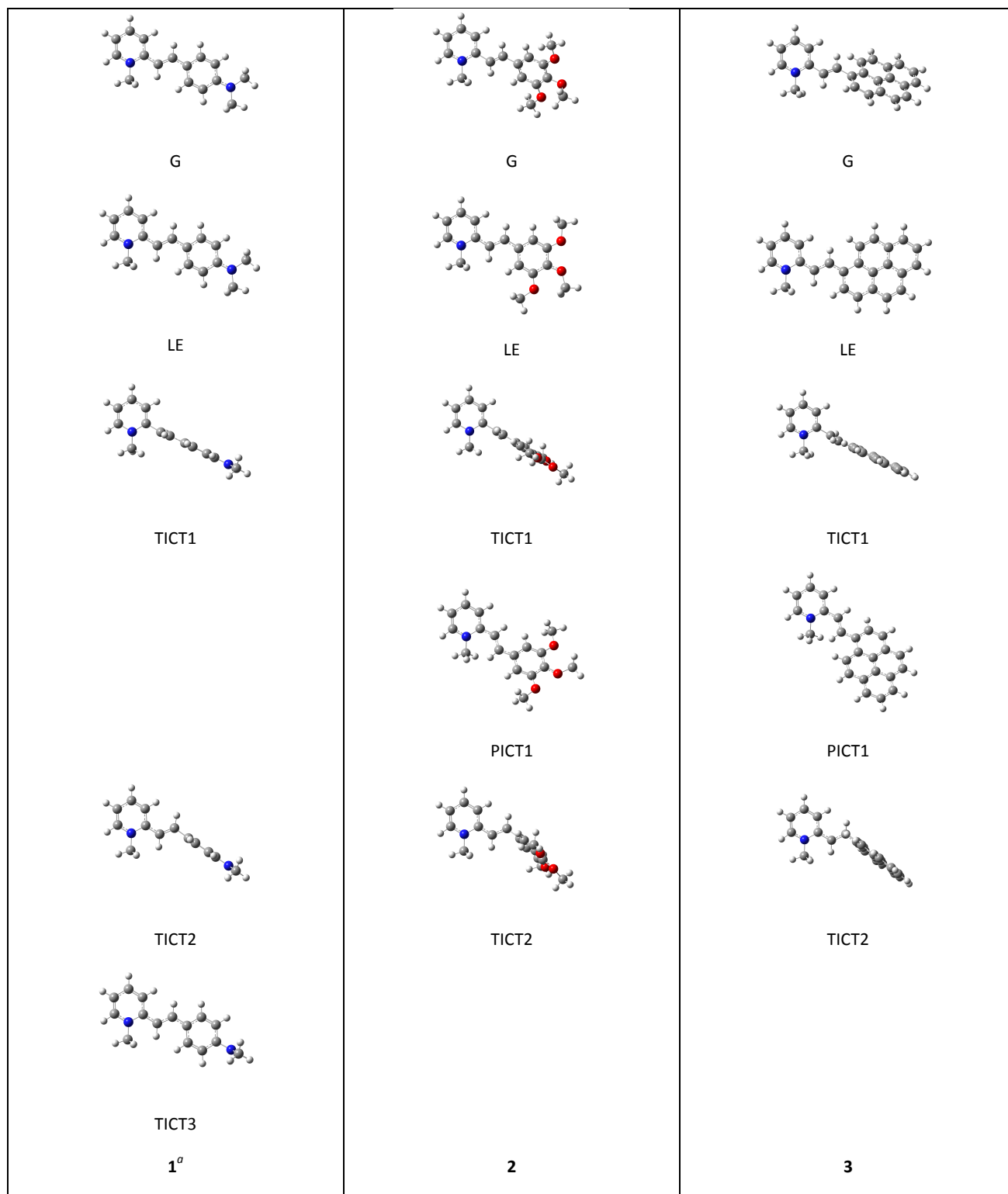
^{a} from ref. 27

Figure 6. Optimised geometries of G and ES (LE, TICT1, PICT1, TICT2 and TICT3) minima of compounds **1**, **2** and **3** in water. Level of theory: (TD-)DFT CAM-B3LYP/SNSD/IEF-PCM(UFF).
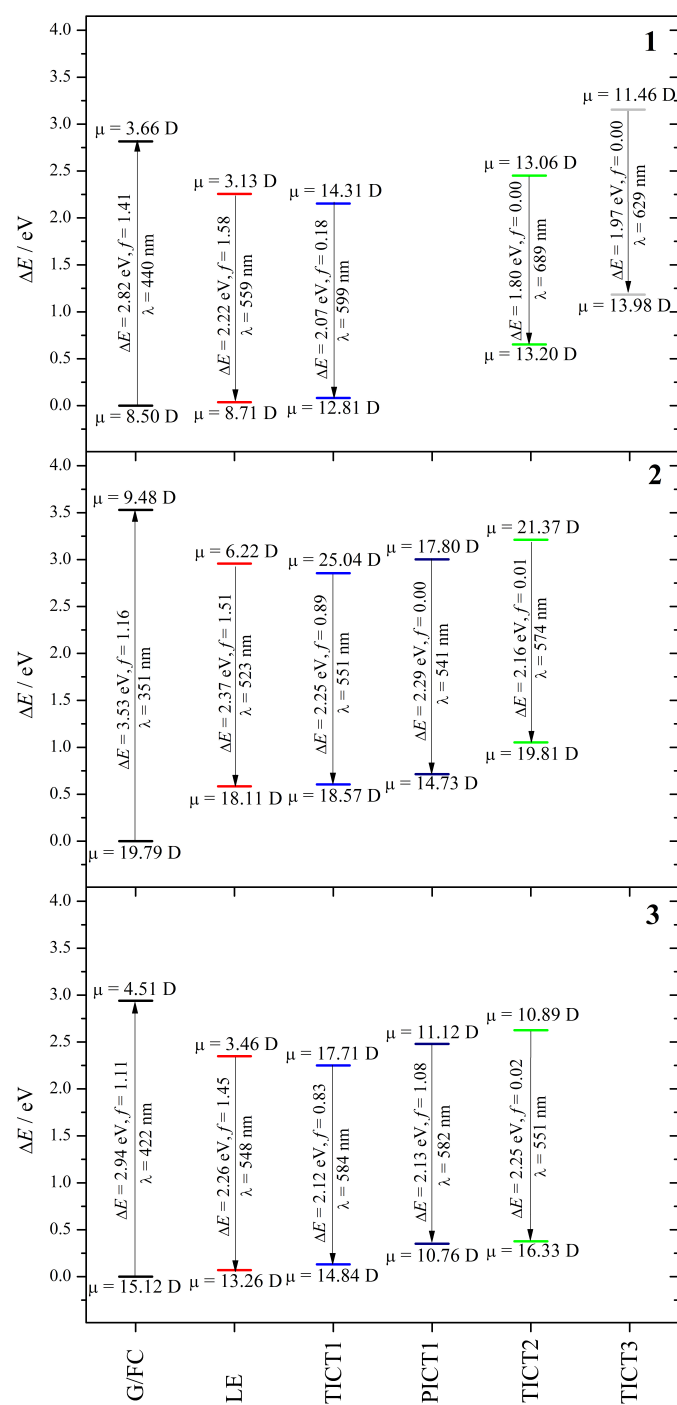
Figure 7. Plots of the energy levels of G and ES (LE, TICT1, PICT1, TICT2 and TICT3) minima of compounds **1**, **2** and **3** in water. Transition energies (in eV), wavelengths (in nm), oscillator strengths, and modulus of electric dipole moments (in D) are also depicted. Plot for compound **1** is elaborated from ref. 27.

Experimental

Photophysical measurements. The investigated compounds were synthesised for previous works. [19,20,37-41] The experimental setup for femtosecond fluorescence up–conversion measurements was widely described elsewhere. [42-44] The 400 nm excitation pulses of ca. 40 fs were generated using an amplified Ti:sapphire laser system (Spectra Physics). In the up–conversion set–up (Halcyone, Ultrafast Systems) the 400 nm pulses excite the sample whereas the remaining fundamental laser beam plays the role of the "optical gate" after passing through a delay line. The fluorescence of the sample is collected and focused onto a BBO crystal together with the delayed fundamental laser beam. The upconverted fluorescence beam is focused into the entrance of a monochromator using a lens, and it is then detected by a photomultiplier connected to a photon counter. The temporal resolution of the up–conversion equipment is about 250 fs, whereas the spectral resolution is 5 nm. Ultrafast spectroscopic data were fitted by Global and Target Analysis using the Glotaran software. [45] The fluorescence up-conversion measurements were carried out on solutions of **2** in pure water and **3** in a water/ethanol mixture 90/10 v/v (a little amount of alcohol was added to aid solubilisation of the bulky pyrenyl derivative), characterised by concentrations of 8.9×10^{-4} and 4.9×10^{-5} M, respectively. The possible occurrence of aggregation of the investigated compounds in these concentrated solutions was ruled out by recording stationary UV-vis absorption spectra in solutions at different concentrations. No concentration effect was found in the case of **2** and **3** in aqueous medium.

Computational details. The molecular geometries of the ground electronic state (G) and of different minima of S_1 (LE and those due to the torsion around the dihedral angles θ1 and θ2) were fully optimised at (TD–)DFT level, both *in vacuo* and in aqueous solution. Harmonic vibrational frequencies of ground and excited electronic states were also computed employing analytical Hessians and finite differences of analytical gradients, respectively. The properties of the first five singlet excited electronic states, their electronic densities, absorption and emission spectra were investigated at TD–DFT level employing different functionals. In particular, we chose global (*viz.* B3LYP[46] and M06–2X)[47] and range-separated (*viz.* CAM–B3LYP[48] and ωB97X)[49] hybrid functionals, coupled with the 6–31+G*, aug–cc–pVDZ,[50-55] and SNSD[56] basis sets. Calculations performed coupling different functionals and basis sets confirm what emerged in previous studies. [21,27,37] For the sake of brevity, only the results obtained at CAM-B3LYP/SNSD level of theory are shown in order to have a direct comparison with those shown in the previous references. The vibronic progressions of the different electronic transitions, both in absorption and in emission, were also simulated, including Duschinsky and Herzberg–Teller effects, in solution. [57-60] Solvent effects were taken into account at the TD–DFT level, by mean of the implicit Polarizable Continuum Model in its Integral Equation Formalism (IEF–PCM). [61,62] The excitation energies were calculated at the TD–DFT level by employing both the standard Linear–Response (LR) and the State–Specific (SS) treatments of solvent effects at the minima

located, both within the non–equilibrium (neq) and equilibrium (eq) solvation regimes.[63-65] The reported data refer to SS solvation models, which is well-known to provide a better description. The use of eq/neq solvation regimes was dedicated to the optimisations and the absorption/emission, respectively. Obviously, the solvation model and regime affect the absolute values of the calculated properties, but for the investigated systems the differences are not so large to derange the described picture. The PCM molecular cavity was built employing scaled Universal Force Field (UFF)[66] *radii*, according to the defaults of the latest implementation of the PCM in the Gaussian package[67] (based on a continuum surface charge formalism). Standard values were employed for the dielectric constants and refractive indexes of the different solvents.

Finally, we remind that the electric dipole moment for a charged species is ill-defined since it depends on the choice of the coordinate origin. However, in Quantum and Computational Chemistry, a "working definition" is commonly assumed, which refers to the centre of the nuclear charge of the system We computed the electric dipole moment for S_n (n = 0, 1, … 5) at the TD–DFT level, employing the above mentioned working definition. The calculations were run using GAUSSIAN 09 code.[67]

Conclusions

Joining state-of-the-art femtosecond resolved fluorescence up-conversion spectroscopy and quantum-mechanical calculations including vibronic effects, it was possible to get a deeper insight into the excited state dynamics of two dipolar cationic dyes (Donor–π–Acceptor[+]), characterised by the same electron deficient methylpyridinium moiety and by different electron donor portions: a trimethoxyphenyl (compound **2**) and a pyrene (compound **3**). In both cases, a multiple emission behaviour was pointed out: the experimental observation of distinct emissive species was related to the presence of different local minima in the potential energy surface of the lowest excited singlet state revealed by the computations. In the case of compound **2**, the Time Resolved Area Normalised Emission Spectra (TRANES) reconstructed from the ultrafast spectroscopic data showed the presence of one isoemissive point, which unambiguously indicates the existence of two emitting species involved in the excited state deactivation (characterised by lifetimes of 1.1 and 28 ps) and allows population dynamics to be distinguished from the occurrence of mere solvation. Quantum Mechanical computations by methods rooted into the Density Functional Theory and its time-dependent extension identified two local minima in S_1 responsible for emissions in excellent agreement with the experimental observations, and defined their structural and electronic properties: the LE state (planar and characterised by a low dipole moment) and the TICT1 state (highly polar and obtained from LE by torsion around the quasi-single bond between the methylpyridinium and the ethene bridge). A more

complex behaviour was instead revealed in the case of the pyrenyl derivative (**3**), for which the ultrafast fluorescence data suggest the involvement of three different emitting states showing lifetimes of 1.0, 40 and 270 ps. The first emitter is the planar and low polar LE state, responsible for a high energetic fluorescence. The second and third local minima retrieved in S_1 are both significantly polar, responsible for similar and red-shifted emissions and described respectively by twisted and planar geometry (TICT1 and PICT1), respectively. These species are generated from the LE state by progressive rotation of the methylpyridinium moiety (to give structures characterised by θ_1 dihedral angle of ca. 90° and 150°, respectively), so that the experimental fluorescence dynamics is adequately reproduced by a consecutive kinetic model (LE→TICT1→PICT1). The emission from PICT1 indeed revealed the presence of an interconversion between conformers in the excited state against the NEER principle. This study clearly showed that structural modifications in the electron donor moiety of cationic push-pull systems can induce strongly different excited state dynamics, which may lead to a variety of possible applications wherein the specific behaviour of a given compound could be advantageously exploited.

Acknowledgments

Notes and references

1 S. R. Marder, *Chem. Commun.*, 2006, 131.
2 F. Terenziani, C. Katan, E. Badaeva, S. Tretiak and M. Blanchard–Desce, *Adv. Mater.*, 2008, **20**, 4641.
3 P. N. Prasad and B. A. Reinhardt, *Chem. Mater.,* 1990, **2**, 660.
4 S. R. Marder, J. W. Perry, C. P. Yakymyshyn, *Chem. Mater.*, 1994, **6**, 1137-1147.
5 B. Strehmel, A. M. Sarker and H. Detert, *ChemPhysChem*, 2003, **4**, 249.
6 C. Rouxel, M. Charlot, Y. Mir, C. Frochot, O. Mongin and M. Blanchard–Desce, *New J. Chem.*, 2011, **35**, 1771.
7 H. Young Woo, B. Liu, B. Kohler, D. Korystov, A. Mikhailovsky and G. C. Bazan, *J. Am. Chem. Soc.*, 2005, **127**, 14721.
8 M. Albota, D. Beljonne, J. Bredas, J. E. Ehrlich, J. Fu, A. A. Heikal, S.E. Hess, T. Kogej, M. D. Levin, S. R. Marder, D. McCord–Maughon, J. W. Perry, H. Rockel, M. Rumi, G. Subramaniam, W. W. Webb, X. Wu and C. Xu, *Science*, 1998, **281**, 1653.
9 A. Abbotto, L. Beverina, R. Bozio, A. Facchetti, C. Ferrante, G. A. Pagani, D. Pedron and R. Signorini, *Chem. Comm.* 2003, 2144.
10 X. M. Wang, Y. F. Zhou, W. T. Yu, C. Wang, Q. Fang, M. H. Jiang, H. Lei and H. Z. Wang, *J. Mater. Chem.*, 2000, **10**, 2698.
11 L. Anatonov, K. Kamada, K. Ohta and F. S. Kamounah, *Phys. Chem. Chem. Phys.*, 2003, **5**, 1193.

12 P. C. Ray and J. Leszczynski, *J. Phys. Chem. A*, 2005, **109**, 6689.

13 O. Rubio-Pons, Y. Luo and H. Agren, *J. Chem. Phys.*, 2006, 124.

14 S. Ciorba, B. Carlotti, I. Skoric, M. Sindler-Kulyk and A. Spalletti, *J. Photochem. Photobiol. A: Chemistry* 2011, **219**, 1.

15 R. Flamini, I. Tomasi, A. Marrocchi, B. Carlotti and A. Spalletti, *J. Photochem. Photobiol. A: Chemistry,* 2011, **223**, 140.

16 B. Carlotti, R. Flamini, A. Spalletti and F. Elisei, *ChemPhysChem,* 2012, **13** (3), 724.

17 B. Carlotti, R. Flamini, I. Kikas, U. Mazzucato and A. Spalletti, *Chem. Phys.*, 2012, **407**, 9.

18 B. Carlotti, I. Kikaš, I. Škorić, A. Spalletti and F. Elisei, *ChemPhysChem,* 2013, **14**, 970.

19 B. Carlotti, G. Consiglio, F. Elisei, C.G. Fortuna, U. Mazzucato and A. Spalletti, *J. Phys. Chem. A,* 2014, **118**, 3580.

20 B. Carlotti, G. Consiglio, F. Elisei, C.G. Fortuna, U. Mazzucato and A. Spalletti, *J. Phys. Chem. A,* 2014, **118**, 7782.

21 B. Carlotti, E. Benassi, V. Barone, G. Consiglio, F. Elisei, A. Mazzoli and A. Spalletti, *ChemPhysChem*, 2015, **16**, 1440.

22 C. G. Fortuna, C. Bonaccorso, F. Qamar, A. Anu, I. Ledoux and G. Musumarra, *Org. Biomol. Chem.*, 2011, **9**, 1608.

23 X. Wang, C. Wang, W. Yu, Y. Zhou, Q. Fang and M. Jiang, *Can. J. Chem.*, 2001, **79**, 174.

24 X. Wang, D. Wang, G. Zhou, W. Yu, Y. Zhou, Q. Fang and M. Jiang, *J. Mater. Chem.*, 2001, **11**, 1600.

25 U. Mazzucato and F. Momicchioli, *Chem. Rev.* 1991, **91**, 1679 and references therein.

26 G. Bartocci, A. Spalletti and U. Mazzucato, Conformational aspects in organic photochemistry, in J. Waluk (Ed.), *Conformational Analysis of Molecules in Excited States*, Wiley-VCH, NewYork, 2000, **ch. 5** and references therein.

27 E. Benassi, B. Carlotti, M. Segado, A. Cesaretti, A. Spalletti, F. Elisei and V. Barone, *J. Phys. Chem. B*, 2015, **119**, 6035.

28 X. Peng, F. Song, E. Lu, Y. Wang, W. Zhou, J. Fan and Y. Gao, *J. Am. Chem. Soc.*, 2005, **127**, 4170.

29 A. Pigliucci, P. Nikolov, A. Rehaman, L. Gagliardi, C. J. Cramer and E. Vauthey, *J. Phys. Chem. A*, 2006, **110**, 9988.

30 B. Wandelt, P. Turkewitsch, B. R. Stranix and G. D. Darling, *J. Chem. Soc. Faraday Trans.*, 1995, **91**, 4199.

31 B. Strehmel, H. Seifert and W. Rettig, *J. Phys. Chem. B,* 1997, **101**, 2232.

32 R. Ramadass and J. Bereiter-Hajn, *J. Phys. Chem. B,* 2007, **111**, 7681.

33 M. L. Horng, J. A. Gardecki, A. Papazyan and M. Maroncelli, *J. Phys. Chem.*, 1995, **99**, 17311.

34 R. Jimenez, G. R. Fleming, P. V. Kuman and M. Maroncelli, *Nature*, 1994, **369**, 471.

35 N. Periasamy and A. S. R. Koti, *Proc. Indian Acad. Sci.*, 2003, **69**, 41.

36 G. Bartocci, S. Ciorba, U. Mazzucato and A. Spalletti *J. Phys. Chem. A*, 2009, **113**, 8557.

37 E. Benassi, B. Carlotti, C. G. Fortuna, V. Barone, F. Elisei and A. Spalletti, *J. Phys. Chem. A,* 2015, **119**, 323.

38 C. G. Fortuna, V. Barresi, C. Bonaccorso, G. Consiglio, S. Failla, A. Trovato–Salinaro and G. Musumarra, *Eur. J. Med. Chem.,* 2012, **47**, 221 and references therein.

39 C. G. Fortuna, G. Forte, V. Pittalà, A. Giuffrida and G. Consiglio, *Comput. Theor. Chem.,* 2012, **985**, 8.

40 A. Cesaretti, B. Carlotti, G. Consiglio, T. Del Giacco, A. Spalletti and F. Elisei, *J. Phys. Chem. B,* 2015, DOI: 10.1021/acs.jpcb.5b02336.

41 A. Cesaretti, B. Carlotti, R. Germani, A. Spalletti and F. Elisei, *Phys. Chem. Chem. Phys.,* accepted for publication.

42 A. Cesaretti, B. Carlotti, P. L. Gentili, C. Clementi, R. Germani and F. Elisei, *Phys. Chem. Chem. Phys.,* 2014, **16**, 23096.

43 A. Cesaretti, B. Carlotti, P. L. Gentili, C. Clementi, R. Germani and F. Elisei, *J. Phys. Chem. B,* 2014, **118**, 8601.

44 B. Carlotti, A. Cesaretti, C. G. Fortuna, A. Spalletti, and F. Elisei, *Phys. Chem. Chem. Phys.,* 2015, **17**, 1877.

45 J. J. Snellenburg, S. Laptenok, R. Seger, K. M. Mullen and I. H. M. van Stokkum, *J. Stat. Software,* 2012, **49**, 1.

46 A. D. Becke, *J. Chem. Phys.,* 1993, **98**, 5648.

47 Y. Zhao and D. G. Truhlar, *Theor. Chem. Acc.,* 2008, **120**, 215.

48 T. Yanai, D. Tew and N. Handy, *Chem. Phys. Lett.,* 2004, **393**, 51.

49 J.–D. Chai and M. Head–Gordon, *Chem. Phys.,* 2008, **128**, 084106.

50 T. H. Dunning Jr., *J. Chem. Phys.,* 1989, **90**, 1007.

51 R. A. Kendall, T. H. Dunning Jr. and R. J. Harrison, *J. Chem. Phys.,* 1992, **96**, 6796.

52 D. E. Woon and T. H. Dunning Jr., *J. Chem. Phys.,* 1993, **98**, 1358.

53 K. A. Peterson, W. E. Woon and T. H. Dunning Jr., *J. Chem. Phys.,* 1994, **100**, 7410.

54 A. K. Wilson, T. van Mourik and T. H. Dunning Jr., *J. Mol. Struct. (Theochem),* 1996, **388**, 339.

55 R. A. Kendall, T. H. Dunning Jr. and R. J. Harrison, *J. Chem. Phys.,* 1992, **96**, 6796.

56 D. E. Woon and T. H. Dunning Jr., *J. Chem. Phys.* 1993, **98**, 1358.

57 http://compchem.sns.it/downloads.

58 R. Improta, V. Barone and F. Santoro, *Angew. Chem., Int. Ed.* 2007, **46**, 405.

59 V. Barone, R. Improta and N. Rega, *Acc. Chem. Res.* 2008, **41**, 605.

60 V. Barone, J. Bloino, M. Biczysko and F. Santoro, *J. Chem. Theory Comput.* 2009, **5**, 540.

61 J. Tomasi, B. Mennucci and E. Cancès, *J. Mol. Struct.: Theochem.* 1999, **464**, 211.

62 G. Scalmani and M. J. Frisch, *J. Chem. Phys.* 2010, **132**, 114110.

63 M. Biczysko, J. Bloino, F. Santoro and V. Barone, in *Computational Strategies for Spectroscopy: From Small Molecules to NanoSystems* (ed. V. Barone), Chap. **8**, Wiley, Chichester, UK, 2011.

64 B. Mennucci, C. Cappelli, C. A. Guido, R. Cammi and J. Tomasi, *J. Phys. Chem. A* 2009, **113**, 3009.

65 R. Improta, V. Barone, G. Scalmani and M. J. Frisch, *J. Chem. Phys.* 2006, **125**, 54103.

66 A. K. Rappé, C. J. Casewit, K. S. Colwell, W. A. Goddard, W. M. Skiff, *J. Am. Chem. Soc.* 1992, **114**, 10024.

67 M. J. Frisch, G. W. Trucks, H. B. Schlegel, G. E. Scuseria, M. A. Robb, J. R. Cheeseman, G. Scalmani, V. Barone, B. Mennucci, G. A. Petersson, *et al.*, *GAUSSIAN09*, Revision D.01, Gaussian, Inc., Wallingford CT, 2009.